ЕЛЕКТРОДИНАМІКА. ПРИСТРОЇ НВЧ ДІАПАЗОНУ. АНТЕННА ТЕХНІКА

UDC 621.396

EIGENMODES ANALYSIS OF SECTORAL COAXIAL RIDGED WAVEGUIDES BY TRANSVERSE FIELD-MATCHING TECHNIQUE. PART 1. THEORY

F. F. Dubrovka, ***Doctor of Engineering, Professor***
S. I. Piltyay, postgraduate student
National Technical University of Ukraine "Kyiv Polytechnic Institute", Kyiv, Ukraine

Аналіз власних хвиль секторних коаксіальних ребристих хвилеводів методом узгодження полів часткових областей. Частина 1. Теорія.

Дубровка Ф. Ф., д.т.н, професор; Пільтяй С. І., аспірант
Національний технічний університет України " Київський політехнічний інститут ", м. Київ, Україна

Ridged structures are widely used in modern waveguide devices. The utilization of ridges enables to create required discontinuities in narrowband devices or to provide wideband matching of hollow waveguides with coaxial transmission lines. Ridged structures are used in filters [1–3], polarizers [4–6], waveguides [7–10], antennas [11–13], orthomode transducers [14–16], lasers [17–19], resonators [20, 21] and other devices.

For development of the devices based on ridged structures it is necessary to know the modal characteristics of ridged waveguides, namely, modes cutoff frequencies and field distributions. The characteristics of ridged waveguides eigenmodes for rectangular cross-section have been analyzed in [22, 23], for square – in [9], for circular – in [23], for elliptical – in [10], for coaxial – in [8]. In [24] the authors of this paper have solved the electrodynamics boundary problem for sectoral coaxial ridged waveguides (SCRW) using integral equation technique (IET), and in [25] their eigenmodes have been analyzed.

In this paper we present the electrodynamics boundary problem solution for the SCRW using transverse field-matching technique (TFMT) to compare complexity, accuracy, convergences for cutoff wave numbers and computing time of these numerical solutions with those obtained by IET.

TE modes

Configurations of hollow infinite SCRW under study and denotations of their cross sectional dimensions are shown in Fig. 1, namely the SCRW with a ridge on the inner wall is shown in Fig. 1*a*, and the SCRW with a ridge on the

outer wall is shown in Fig. 1*b* (hereinafter referred to as subscripts "in" and "out" respectively).

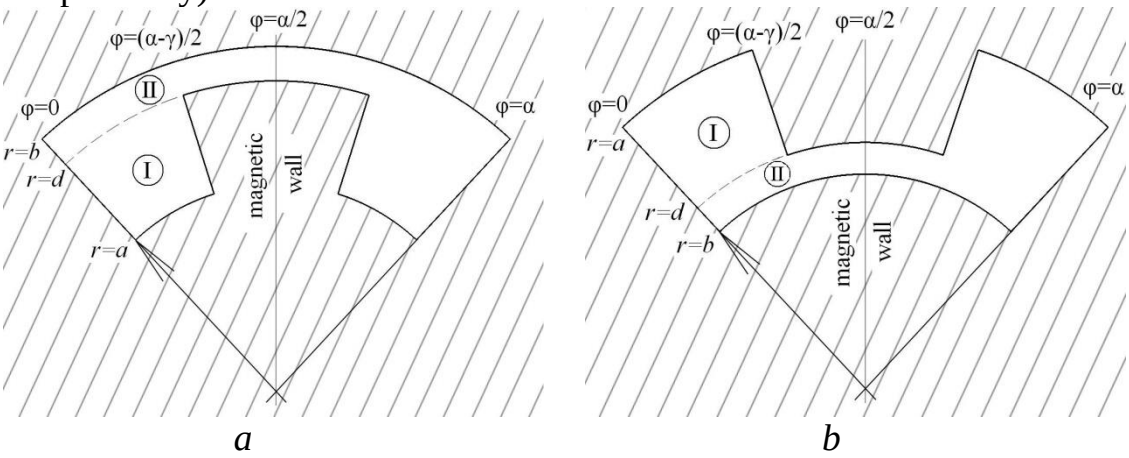

Fig. 1. SCRW configurations and denotations of their cross sections dimensions

Only the modes, for which the SCRW symmetry plane is a magnetic wall, will be investigated. For these modes we represent the fields H_z and E_φ in the regions I and II in the form of infinite sums of the partial modes with unknown amplitudes and cutoff wave numbers, each of which satisfies the Maxwell equations in the cylindrical coordinate system and boundary conditions at the magnetic wall and perfectly conducting walls of SCRW:

$$H_z^{\mathrm{I}}(r,\varphi)=\sum_{n=0}^{\infty}A_n\cos(l_1(n)\varphi)\left[J'_{l_1(n)}(k_c a)Y_{l_1(n)}(k_c r)-Y'_{l_1(n)}(k_c a)J_{l_1(n)}(k_c r)\right], \quad (1)$$

$$H_z^{\mathrm{II}}(r,\varphi)=\sum_{m=0}^{\infty}B_m\cos(l_2(m)\varphi)\left[J'_{l_2(m)}(k_c b)Y_{l_2(m)}(k_c r)-Y'_{l_2(m)}(k_c b)J_{l_2(m)}(k_c r)\right], \quad (2)$$

$$E_\varphi^{\mathrm{I}}(r,\varphi)=Z(f,k_c)\sum_{n=0}^{\infty}A_n\cos(l_1(n)\varphi)\left[J'_{l_1(n)}(k_c a)Y'_{l_1(n)}(k_c r)-Y'_{l_1(n)}(k_c a)J'_{l_1(n)}(k_c r)\right], \quad (3)$$

$$E_\varphi^{\mathrm{II}}(r,\varphi)=Z(f,k_c)\sum_{m=0}^{\infty}B_m\cos(l_2(m)\varphi)\left[J'_{l_2(m)}(k_c b)Y'_{l_2(m)}(k_c r)-Y'_{l_2(m)}(k_c b)J'_{l_2(m)}(k_c r)\right], \quad (4)$$

where A_n and B_m are unknown amplitude coefficients, $l_1(n)=2\pi n/(\alpha-\gamma)$, $l_2(m)=\pi(2m+1)/\alpha$, $J_l(x)$, $Y_l(x)$, $J'_l(x)$, $Y'_l(x)$ are Bessel functions of the first and the second kind and their derivatives, k_c is a cutoff wave number, $Z(f,k_c)=2\pi i f\mu_{ab}/k_c$, where i is an imaginary unit, f is frequency, μ_{ab} is absolute permeability of SCRW inner medium.

Boundary conditions at the interface between regions I and II are as follows:

$$E_\varphi^{\mathrm{II}}\left(r=d,\varphi\in[0;(\alpha-\gamma)/2]\right)=E_\varphi^{\mathrm{I}}\left(r=d,\varphi\in[0;(\alpha-\gamma)/2]\right), \quad (5)$$

$$H_z^{\mathrm{II}}\left(r=d,\varphi\in[0;(\alpha-\gamma)/2]\right)=H_z^{\mathrm{I}}\left(r=d,\varphi\in[0;(\alpha-\gamma)/2]\right). \quad (6)$$

Besides at the perfectly conducting surface of the ridge at $r=d$ and $\varphi\in[(\alpha-\gamma)/2;\alpha/2]$:

$$E_\varphi^{\mathrm{II}}\left(r=d,\varphi\in[(\alpha-\gamma)/2;\alpha/2]\right)=0. \quad (7)$$

Substituting (1)–(4) in (5)–(7) we obtain:

$$\sum_{m=0}^{\infty} B_m \cos(l_2(m)\varphi) J'Y'(l_2(m), k_c b, k_c d) = \sum_{n=0}^{\infty} A_n \cos(l_1(n)\varphi) J'Y'(l_1(n), k_c a, k_c d),$$
$$\varphi \in [0; (\alpha-\gamma)/2], \quad (8)$$

$$\sum_{m=0}^{\infty} B_m \cos(l_2(m)\varphi) J'Y(l_2(m), k_c b, k_c d) = \sum_{n=0}^{\infty} A_n \cos(l_1(n)\varphi) J'Y(l_1(n), k_c a, k_c d),$$
$$\varphi \in [0; (\alpha-\gamma)/2], \quad (9)$$

$$\sum_{m=0}^{\infty} B_m \cos(l_2(m)\varphi) J'Y'(l_2(m), k_c b, k_c d) = 0, \quad \varphi \in [(\alpha-\gamma)/2; \alpha/2], \quad (10)$$

where $J'Y(l,x,y) = J_l'(x)Y_l(y) - Y_l'(x)J_l(y)$, $J'Y'(l,x,y) = J_l'(x)Y_l'(y) - Y_l'(x)J_l'(y)$.

After multiplying left and right parts of the equation (8) by the functions $\cos(l_1(p)\varphi)$, $p = 0, 1, 2, \ldots$, and integrating the result at the interval $[0; (\alpha-\gamma)/2]$, at which the system of these functions is orthogonal, we obtain

$$\sum_{m=0}^{\infty} B_m I_1(p,m) J'Y'(l_2(m), k_c b, k_c d) = A_p \frac{\alpha-\gamma}{4}(1+\delta_{p0}) J'Y'(l_1(p), k_c a, k_c d), \quad (11)$$

from whence it follows, that the amplitude of the p-th partial mode in region I

$$A_p = \frac{4\sum_{m=0}^{\infty} B_m I_1(p,m) J'Y'(l_2(m), k_c b, k_c d)}{(\alpha-\gamma)(1+\delta_{p0}) J'Y'(l_1(p), k_c a, k_c d)}. \quad (12)$$

In (11), (12) δ_{p0} is Kronecker delta, $I_1(p,m) = \int_0^{(\alpha-\gamma)/2} \cos(l_2(m)\varphi)\cos(l_1(p)\varphi)\mathrm{d}\varphi =$

$$= \frac{\alpha-\gamma}{4}\left\{\mathrm{sinc}\left[(2m+1)\frac{\alpha-\gamma}{2\alpha} - p\right] + \mathrm{sinc}\left[(2m+1)\frac{\alpha-\gamma}{2\alpha} + p\right]\right\}, \quad \text{where}$$

$\mathrm{sinc}(x) = \sin(\pi x)/(\pi x)$.

In the same way from (9) the amplitude of the p-th partial mode in region I

$$A_p = \frac{4\sum_{m=0}^{\infty} B_m I_1(p,m) J'Y(l_2(m), k_c b, k_c d)}{(\alpha-\gamma)(1+\delta_{p0}) J'Y(l_1(p), k_c a, k_c d)}. \quad (13)$$

Having equated (12) to (13) one easily obtains

$$\sum_{m=0}^{\infty} B_m I_1(p,m)\left[\frac{J'Y'(l_2(m), k_c b, k_c d)}{J'Y'(l_1(p), k_c a, k_c d)} - \frac{J'Y(l_2(m), k_c b, k_c d)}{J'Y(l_1(p), k_c a, k_c d)}\right] = 0. \quad (14)$$

By introducing designation

$$F_1(p,m,x,y,z) = I_1(p,m)\left[\frac{J'Y'(l_2(m), y, z)}{J'Y'(l_1(p), x, z)} - \frac{J'Y(l_2(m), y, z)}{J'Y(l_1(p), x, z)}\right]$$

and simplifying the expression (14) we obtain

$$\sum_{m=0}^{\infty} B_m F_1(p, m, k_c a, k_c b, k_c d) = 0, \quad p = 0, 1, 2, \ldots \tag{15}$$

Next we multiply left and right parts of the equation (10) by the functions $\cos(l_2(q)\varphi)$, $q = 0, 1, 2, \ldots$, and integrate the result at the interval $[(\alpha-\gamma)/2; \alpha/2]$ and obtain

$$\sum_{m=0}^{\infty} B_m I_2(q, m) J'Y'(l_2(m), k_c b, k_c d) = 0, \tag{16}$$

where $I_2(q,m) = \int\limits_{(\alpha-\gamma)/2}^{\alpha/2} \cos(l_2(m)\varphi)\cos(l_2(q)\varphi)\mathrm{d}\varphi = \frac{\alpha}{4}\delta_{mq} - \frac{\alpha-\gamma}{4}\left\{\mathrm{sinc}\left[(m-q)\frac{\alpha-\gamma}{\alpha}\right] + \right.$

$\left. + \mathrm{sinc}\left[(m+q+1)\frac{\alpha-\gamma}{\alpha}\right]\right\}$.

By introducing designation

$$F_2(q, m, y, z) = I_2(q, m) J'Y'(l_2(m), y, z)$$

we simplify the expression (16) to the following equation

$$\sum_{m=0}^{\infty} B_m F_2(q, m, k_c b, k_c d) = 0, \quad q = 0, 1, 2, \ldots \tag{17}$$

Having united the systems of equations (15), (17) and placing a limit on amount of partial modes in the region II, we obtain the following homogeneous system of linear algebraic equations (SLAE) with unknown partial modes amplitudes B_m:

$$\begin{cases} \sum\limits_{m=0}^{M-1} B_m F_1(p, m, k_c a, k_c b, k_c d) = 0, & p = 0, 1, \ldots (P-1), \\ \sum\limits_{m=0}^{M-1} B_m F_2(q, m, k_c b, k_c d) = 0, & q = 0, 1, \ldots (M-P-1). \end{cases} \tag{18}$$

At the fixed amount of partial modes M the amount of equations of the first type is defined by angular widths ratio of regions I and II [26]: $P = [M(\alpha-\gamma)/\alpha]$, where integer part rounded up or down is designated by [ ].

By rewriting the SLAE (18) in the matrix form we obtain:

$$\begin{bmatrix} F_{0,0} & \cdots & F_{0,M-1} \\ \vdots & \ddots & \vdots \\ F_{M-1,0} & \cdots & F_{M-1,M-1} \end{bmatrix} \cdot \begin{bmatrix} B_0 \\ \vdots \\ B_{M-1} \end{bmatrix} = \begin{bmatrix} 0 \\ \vdots \\ 0 \end{bmatrix}. \tag{19}$$

The elements of the matrix $[F]$ are equal

$$F(i, j) = \begin{cases} F_1(i, j, k_c a, k_c b, k_c d), & i = 0, 1, \ldots (P-1), \\ F_2((i-P), j, k_c b, k_c d), & i = P, (P+1), \ldots (M-1). \end{cases}$$

The condition of nontrivial solution of the homogeneous SLAE (19) is the equality to zero of the matrix $[F]$ determinant. From this condition we define

TE modes cutoff wave numbers. The cutoff wave numbers calculated are to be substituted in homogeneous SLAE (19). Let $B_0 = 1$. Then

$$\begin{bmatrix} F_{0,1} & \cdots & F_{0,M-1} \\ \vdots & \ddots & \vdots \\ F_{M-2,1} & \cdots & F_{M-2,M-1} \end{bmatrix} \cdot \begin{bmatrix} B_1 \\ \vdots \\ B_{M-1} \end{bmatrix} = -\begin{bmatrix} F_{0,0} \\ \vdots \\ F_{M-2,0} \end{bmatrix}; \quad \begin{bmatrix} B_1 \\ \vdots \\ B_{M-1} \end{bmatrix} = -\begin{bmatrix} F_{0,1} & \cdots & F_{0,M-1} \\ \vdots & \ddots & \vdots \\ F_{M-2,1} & \cdots & F_{M-2,M-1} \end{bmatrix}^{-1} \cdot \begin{bmatrix} F_{0,0} \\ \vdots \\ F_{M-2,0} \end{bmatrix}$$

Consequently, all partial modes amplitudes B_m have been defined. After this we define the partial modes amplitudes A_p by the formula (12) or (13). The distribution of longitudinal component of magnetic field H_z we define by the formulas (1), (2). Transversal components of magnetic and electric fields we define using the longitudinal and transversal field components connection formulas.

TM modes

The TM modes designations introduced in this section coincide with the ones given above for TE modes, but they refer only to TM modes. For TM modes we represent the fields E_z and H_φ in the regions I and II (Fig. 1) in the form of infinite sums of the partial modes with unknown amplitudes and cutoff wave numbers, each of which satisfies the Maxwell equations in the cylindrical coordinate system and boundary conditions at the magnetic wall and perfectly conducting walls of SCRW:

$$E_z^{\mathrm{I}}(r,\varphi) = \sum_{n=0}^{\infty} A_n \sin(l_1(n)\varphi)\left[J_{l_1(n)}(k_c a)Y_{l_1(n)}(k_c r) - Y_{l_1(n)}(k_c a)J_{l_1(n)}(k_c r)\right], \quad (20)$$

$$E_z^{\mathrm{II}}(r,\varphi) = \sum_{m=0}^{\infty} B_m \sin(l_2(m)\varphi)\left[J_{l_2(m)}(k_c b)Y_{l_2(m)}(k_c r) - Y_{l_2(m)}(k_c b)J_{l_2(m)}(k_c r)\right], \quad (21)$$

$$H_\varphi^{\mathrm{I}}(r,\varphi) = Y(f,k_c)\sum_{n=0}^{\infty} A_n \sin(l_1(n)\varphi)\left[J_{l_1(n)}(k_c a)Y'_{l_1(n)}(k_c r) - Y_{l_1(n)}(k_c a)J'_{l_1(n)}(k_c r)\right], \quad (22)$$

$$H_\varphi^{\mathrm{II}}(r,\varphi) = Y(f,k_c)\sum_{m=0}^{\infty} B_m \sin(l_2(m)\varphi)\left[J_{l_2(m)}(k_c b)Y'_{l_2(m)}(k_c r) - Y_{l_2(m)}(k_c b)J'_{l_2(m)}(k_c r)\right], \quad (23)$$

where A_n and B_m are unknown amplitude coefficients, $l_1(n) = 2\pi(n+1)/(\alpha-\gamma)$, $l_2(m) = \pi(2m+1)/\alpha$, $J_l(x)$, $Y_l(x)$, $J'_l(x)$, $Y'_l(x)$ are Bessel functions of the first and the second kind and their derivatives, k_c is a cutoff wave number, $Y(f,k_c) = 2\pi i f\varepsilon_{ab}/k_c$, where i is an imaginary unit, f is frequency, ε_{ab} is absolute permittivity of SCRW inner medium.

Boundary conditions at the interface between regions I and II are as follows:

$$E_z^{\mathrm{II}}\left(r=d, \varphi\in[0;(\alpha-\gamma)/2]\right) = E_z^{\mathrm{I}}\left(r=d, \varphi\in[0;(\alpha-\gamma)/2]\right), \quad (24)$$

$$H_\varphi^{\mathrm{II}}\left(r=d, \varphi\in[0;(\alpha-\gamma)/2]\right) = H_\varphi^{\mathrm{I}}\left(r=d, \varphi\in[0;(\alpha-\gamma)/2]\right). \quad (25)$$

Besides, at the perfectly conducting surface of the ridge at $r=d$ and $\varphi\in[(\alpha-\gamma)/2;\alpha/2]$:

$$E_z^{\mathrm{II}}\left(r=d, \varphi\in[(\alpha-\gamma)/2;\alpha/2]\right) = 0. \quad (26)$$

Next we substitute (20)–(23) in (24)–(26):

$$\sum_{m=0}^{\infty} B_m \sin(l_2(m)\varphi) JY(l_2(m), k_c b, k_c d) = \sum_{n=0}^{\infty} A_n \sin(l_1(n)\varphi) JY(l_1(n), k_c a, k_c d),$$
$$\varphi \in [0; (\alpha-\gamma)/2], \quad (27)$$

$$\sum_{m=0}^{\infty} B_m \sin(l_2(m)\varphi) JY'(l_2(m), k_c b, k_c d) = \sum_{n=0}^{\infty} A_n \sin(l_1(n)\varphi) JY'(l_1(n), k_c a, k_c d),$$
$$\varphi \in [0; (\alpha-\gamma)/2], \quad (28)$$

$$\sum_{m=0}^{\infty} B_m \sin(l_2(m)\varphi) JY(l_2(m), k_c b, k_c d) = 0, \quad \varphi \in [(\alpha-\gamma)/2; \alpha/2]. \quad (29)$$

where $JY(l,x,y) = J_l(x)Y_l(y) - Y_l(x)J_l(y)$, $JY'(l,x,y) = J_l(x)Y_l'(y) - Y_l(x)J_l'(y)$.

After multiplying left and right parts of the equation (27) by the functions $\sin(l_1(p)\varphi)$, $p = 0, 1, 2, \ldots$, and integrate the result at the interval $[0; (\alpha-\gamma)/2]$, at which the system of these functions is orthogonal, we obtain

$$\sum_{m=0}^{\infty} B_m I_1(p,m) JY(l_2(m), k_c b, k_c d) = A_p \frac{\alpha-\gamma}{4} JY(l_1(p), k_c a, k_c d), \quad (30)$$

from whence it follows, that the amplitude of the p-th partial mode in region I

$$A_p = \frac{4\sum_{m=0}^{\infty} B_m I_1(p,m) JY(l_2(m), k_c b, k_c d)}{(\alpha-\gamma) JY(l_1(p), k_c a, k_c d)}. \quad (31)$$

In (30), (31)

$$I_1(p,m) = \int_0^{(\alpha-\gamma)/2} \sin(l_2(m)\varphi)\sin(l_1(p)\varphi)\,\mathrm{d}\varphi = \frac{\alpha-\gamma}{4}\left\{\operatorname{sinc}\left[(2m+1)\frac{\alpha-\gamma}{2\alpha} - (p+1)\right] - \right.$$
$$\left. - \operatorname{sinc}\left[(2m+1)\frac{\alpha-\gamma}{2\alpha} + (p+1)\right]\right\}.$$

In the same way from (28) the amplitude of the p-th partial mode in region I

$$A_p = \frac{4\sum_{m=0}^{\infty} B_m I_1(p,m) JY'(l_2(m), k_c b, k_c d)}{(\alpha-\gamma) JY'(l_1(p), k_c a, k_c d)}. \quad (32)$$

Having equated (31) to (32) one easily obtains

$$\sum_{m=0}^{\infty} B_m I_1(p,m)\left[\frac{JY(l_2(m), k_c b, k_c d)}{JY(l_1(p), k_c a, k_c d)} - \frac{JY'(l_2(m), k_c b, k_c d)}{JY'(l_1(p), k_c a, k_c d)}\right] = 0. \quad (33)$$

After this we introduce the following designation

$$F_1(p,m,x,y,z) = I_1(p,m)\left[\frac{JY(l_2(m), y, z)}{JY(l_1(p), x, z)} - \frac{JY'(l_2(m), y, z)}{JY'(l_1(p), x, z)}\right].$$

Using this designation (33) can be rewritten by the formula (15).

Next we multiply left and right parts of the equation (29) by the functions $\sin(l_2(q)\varphi)$, $q = 0, 1, 2, \ldots$, and integrate the result at the interval $[(\alpha-\gamma)/2; \alpha/2]$ and obtain

$$\sum_{m=0}^{\infty} B_m I_2(q,m) JY(l_2(m), k_c b, k_c d) = 0, \qquad (34)$$

where $I_2(q,m) = \int\limits_{(\alpha-\gamma)/2}^{\alpha/2} \sin(l_2(m)\varphi)\sin(l_2(q)\varphi)\mathrm{d}\varphi = \frac{\alpha}{4}\delta_{mq} - \frac{\alpha-\gamma}{4}\left\{\mathrm{sinc}\left[(m-q)\frac{\alpha-\gamma}{\alpha}\right] - \right.$

$$\left. - \mathrm{sinc}\left[(m+q+1)\frac{\alpha-\gamma}{\alpha}\right]\right\}.$$

Next we introduce the following designation

$$F_2(q,m,y,z) = I_2(q,m) JY(l_2(m), y, z).$$

Using this designation (34) can be rewritten by the formula (17).

Further solution for TM modes is the same as for TE ones.

Solutions convergence for cutoff wave numbers

Now we carry out cutoff wave numbers convergence analysis depending on the amount of partial modes M limiting the sums in (18) for both configurations of SCRW (Fig. 1). As one can see in Fig. 1 the region I is limited by three perfectly conducting walls of SCRW and the interface, and region II is limited by one magnetic wall, three perfectly conducting walls and the interface for both configurations. Therefore all formulas remain the same for both constructions. For the SCRW with a ridge on an inner wall we set dimensions ratios and angles as follows: $\alpha = 86°$, $\gamma = 30°$, $a/b = 0.5$, $(d-a)/b = 0.4$. For the SCRW with a ridge on an outer wall the dimensions ratios and angles are as follows: $\alpha = 86°$, $\gamma = 30°$, $b/a = 0.5$, $(a-d)/a = 0.4$. Residual errors ($\delta = \frac{[k_c(M) - k_c(30)]}{k_c(30)} \times$ $\times 100\%$) plots for cutoff wave numbers of first four modes of SCRW versus the number of partial modes M are shown in Fig. 2. Herewith residual errors for the first, the second, the third TE modes and for the first TM mode are shown by solid, dashed, dash-dotted and dotted lines respectively. The results for SCRW with a ridge on an inner wall are shown in Fig. 2*a*, and for SCRW with a ridge on an outer wall – in Fig. 2*b*. The residual errors are calculated relative to the cutoff wave numbers obtained at $M = 30$.

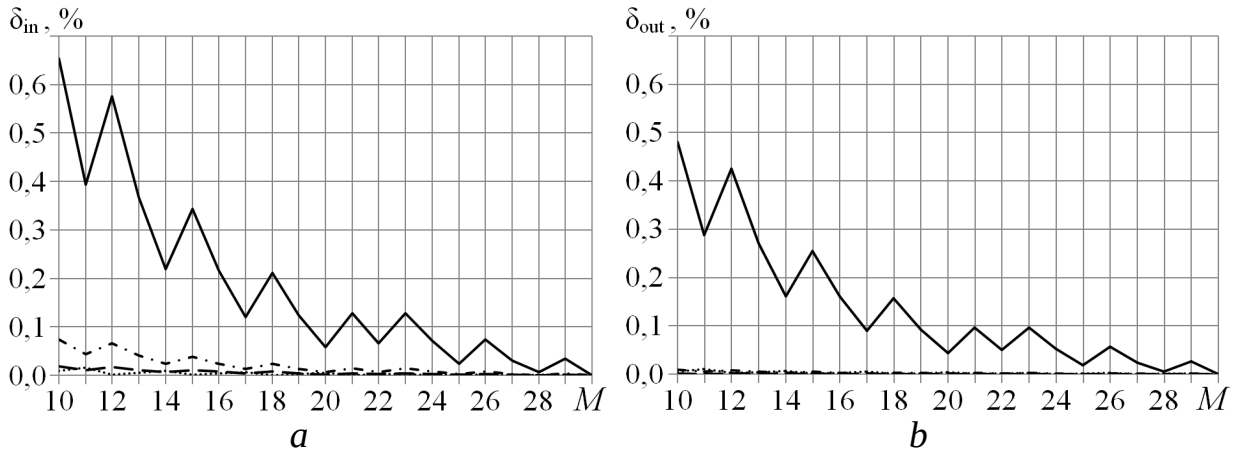

Fig. 2. Cutoff wave numbers residual errors

As one can see in Fig. 2 taking into account 24 partial modes provides the residual errors of cutoff wave numbers of first four modes less than 0.1% comparatively with the values of cutoff wave numbers under 30 partial modes. Therefore, one concludes that it is enough to take into account 24 partial modes for the calculation of SCRW cutoff wave numbers for both configurations by TFMT with residual error less than 0.1%. It has been shown in [24] that for the calculation of cutoff wave numbers of SCRW by IET with residual error less than 0.1% it is enough to utilize 3 orthogonal basis functions, which correctly take into account singular field behavior at the ridge, and 15 partial modes. Besides it is worth to be mentioned that at cutoff wave numbers residual error less than 0.1% computing time in the case of IET is 5 times less than the computing time in the case of TFMT.

Conclusions

The electrodynamics eigenmodes boundary problem for sectoral coaxial single-ridged waveguides has been solved by TFMT. The formulas obtained provide possibilities to compute cutoff wave numbers and electric and magnetic fields distributions of TE and TM modes in the presence of the ridge either on the inner or on the outer wall of the waveguide. It has been shown that for calculation of cutoff wave numbers with residual error less than 0.1% it is enough to utilize 24 partial modes, herewith computing time in the case of IET is 5 times less than the computing time in the case of TFMT.

References

1. Suntheralingam N., Mohottige N., Budimir D. Electromagnetic modelling of ridged waveguide resonator loaded bandpass filters // 2010 IEEE Antennas and Propagation Society International Symposium (APSURSI 2010), Toronto, Canada, 2010, pp. 1–4.

2. Li S., Fu J., Wu X. Double ridged waveguide low pass filters for satellite application // 2007 International Symposium on Microwave, Antenna, Propagation and EMC Technologies for Wireless Communications, Hangzhou, China, 2007, pp. 408–410.

3. Manuilov M. B., Kobrin K. V., Obrezanova L. A. Ridged waveguide filters with improved performance // 16th International Crimean Conference on Microwave and Telecommunication Technology (CriMiCo 2006), Sevastopol, Ukraine, 2006, pp. 507–508.

4. Dai D., Wang Z., Julian N., Bowers J. E. Compact broadband polarizer based on shallowly-etched silicon-on-insulator ridge optical waveguides // 2011 Optical Fiber Communication and National Fiber Optic Engineers Conference (OFC/NFOEC), Los Angeles, USA, 2011, pp. 1–3.

5. Tribak A., Mediavilla A., Cano J. L., Boussouis M., Cepero K. Ultra-broadband low axial ratio corrugated quad-ridge polarizer // European Microwave Conference (EuMC 2009), Rome, Italy, 2009, pp. 73–76.

6. Bull J. D., Kato H., Jaeger N. Asymmetrically strained ridge waveguide for passive polarization conversion // IEEE Photonics Technology Letters. – Dec. 2008.– vol. 20, № 24. – pp. 2186–2188.

7. Polemi A., Maci S., Kildal P.-S. Dispersion characteristics of a metamaterial-based parallel-plate ridge gap waveguide realized by bed of nails // IEEE Trans. Antennas Propagat. – March 2011. – vol. 59, № 3 – pp. 904–913.

8. Ruiz-Bernal M. A., Valverde-Navarro M., Goussetis G., Gomez-Tornero J.-L., Feresidis A. P. Higher order modes of the ridged coaxial waveguide // 36th European Microwave Conference, Manchester, UK, 2006, pp. 1221–1224.

9. Tang Y., Zhao J., Wu W. Analysis of quadruple-ridged square waveguide by multilayer perceptron neural network model // Asia-Pacific Microwave Conference (APMC 2006), Yokohama, Japan, 2006, pp. 1912–1918.

10. Xu J., Wang W., Gong Y., Wei Y. Analysis of elliptical ridged waveguide // Joint 31st International Conference on Infrared Millimeter Waves and 14th International Conference on Teraherz Electronics (IRMMW-THz 2006), Shanghai, China, 2006, p. 265.

11. Jacobs O. B., Odendaal J. W., Joubert J. Elliptically shaped quad-ridge horn antennas as feed for a reflector // IEEE Antennas Wireless Propagat. Lett.–2011.–vol. 10.–pp. 756–759.

12. Akgiray A., Weinreb S., Imbriale W. Design and measurements of dual-polarized wideband constant-beamwidth quadruple-ridged flared horn // 2011 IEEE International Symposium on Antennas and Propagation (APSURSI 2011), Spokane, USA, 2011, pp. 1135–1138.

13. Jacobs O. B., Odendaal J. W., Joubert J. Quad ridge horn antenna with elliptically shaped sidewalls // 2011 International Conference on Electromagnetics in Advanced Applications (ICEAA 2011), Torino, Italy, 2011, pp. 259–262.

14. Coutts G. M. Wideband diagonal quadruple-ridge orthomode transducer for circular polarization detection // IEEE Trans. AP. – June 2011. – vol. 59, № 6 – pp. 1902–1909.

15. Hwang J.-H., Oh Y. Compact orthomode transducer using single-ridged triangular waveguides // IEEE Microwave Wireless Comp. Lett. – 2011. – vol. 21, № 8 – pp. 412–414.

16. Zhang H. Z. A wideband orthogonal-mode junction using ridged sectoral waveguides // 2002 IEEE Int. Antennas Propagat. Symp. Dig. – June 2002. – vol. 40. – pp. 432–435.

17. Yeo C. I., Jang S. J., Yu J. S., Lee Y. T. 1.3-μm laterally tapered ridge waveguide DFB lasers with second-order Cr surface gratings // IEEE Photonics Technology Letters. – Nov. 2010. – vol. 22, № 22. – pp. 1668–1670.

18. Price R. K., Verma V. B., Elarde V. C., Coleman J. J. Internal loss, modal characteristics, and bend loss of asymmetric cladding ridge waveguide lasers at 850 nm // Journal of Applied Physics. – Jan. 2008. – vol. 103, № 1. – pp. 013108–013108-6.

19. Teng J. H., Lim E. L., Chua S. J., Ang S. S., Chong L. F., Dong J. R., Yin R. Self-aligned metal-contact and passivation technique for submicron ridge waveguide laser fabrication // J. of Vac. Sci. & Tech. B: Microel. and nm Struct.–2008.–vol.26, № 5.–pp.1748–1752.

20. Amadjikpe A. L., Papapolymerou J. A high-Q electronically tunable evanescent-mode double-ridged rectangular waveguide resonator // 2008 IEEE Int. Microwave Symp. Dig. – June 2008. – pp. 1019–1022.

21. Serebryannikov A. E., Vasylchenko O. E., Schunemann K. Fast coupled-integral-equations-based analysis of azimuthally corrugated cavities // IEEE Microwave Wireless Comp. Lett. – May 2004. – vol. 14, № 5. – pp. 240–242.

22. Jarvis D. A., Rao T. C. Design of double-ridged rectangular waveguide of arbitrary aspect ratio and ridge height // IEE Proc. AP. – Feb. 2000. – vol. 147, № 1. – pp. 31–34.

23. Rong Y., Zaki K. A. Characteristics of generalized rectangular and circular ridge waveguides // IEEE Trans. Microwave Theory Tech. – Feb. 2000. – vol. 48, № 2.– pp. 258–265.

24. Dubrovka F. F., Piltyay S. I. Electrodynamics boundary problem solution for sectoral coaxial ridged waveguides by integral equation technique // Radioelectronics and Communications Systems. – May 2012. – vol. 55, № 5. – pp. 191–203.

25. Dubrovka F. F., Piltyay S. I. Eigenmodes of sectoral coaxial ridged waveguides // Radioelectronics and Communications Systems. – June 2012. – vol. 55, № 6. – pp. 239–247.

26. Mittra R., Lee S. W. Analytical Techniques in the Theory of Guided Waves. New York: Macmillan, 1971. – 302 p.

Дубровка Ф. Ф., Пільтяй С. І. ***Аналіз власних хвиль секторних коаксіальних ребристих хвилеводів методом узгодження полів часткових областей. Частина 1. Теорія.*** *Методом узгодження полів часткових областей розв'язано крайову задачу електродинаміки для власних хвиль секторних коаксіальних одноребернх хвилеводів. Отримані формули дозволяють розрахувати критичні хвильові числа та розподіли електричного та магнітного полів ТЕ та ТМ мод при наявності ребра на внутрішній чи зовнішній стінці хвилеводу. Проведено аналіз збіжності розв'язків для критичних хвильових чисел в залежності від кількості парціальних мод. Показано, що для отримання залишкової похибки розрахунку критичних хвильових чисел, меншої за 0,1%, потрібно використовувати 24 парціальні моди.*

Ключові слова: *крайова задача електродинаміки, секторний коаксіальний ребристий хвилевід, метод узгодження полів часткових областей, власні хвилі типу ТЕ, власні хвилі типу ТМ, збіжність розв'язків, залишкова похибка.*

Дубровка Ф. Ф., Пильтяй С. И. ***Анализ собственных волн секторных коаксиальных ребристых волноводов методом согласования полей частичных областей. Часть 1. Теория.*** *Методом согласования полей частичных областей решена краевая задача электродинамики для собственных волн секторных коаксиальных одноребернх волноводов. Приведенные формулы позволяют рассчитать критические волновые числа и распределения электрического и магнитного полей ТЕ и ТМ мод при наличии ребра на внутренней или внешней стенке волновода. Проведен анализ сходимости решений для критических волновых чисел в зависимости от количества парциальных мод. Показано, что для получения остаточной погрешности расчета критических волновых чисел, меньшей 0,1%, необходимо использовать 24 парциальные моды.*

Ключевые слова: *краевая задача электродинамики, секторный коаксиальный ребристый волновод, метод согласования полей частичных областей, собственные волны типа ТЕ, собственные волны типа ТМ, сходимость решений, остаточная погрешность.*

Dubrovka F. F., Piltyay S. I. ***Eigenmodes analysis of sectoral coaxial ridged waveguides by transverse field-matching technique. Part 1. Theory.***

Introduction. The utilization of ridged structures in modern waveguide devises is discussed. The goals of the research presented in the paper are defined.

TE modes. The geometrical configurations of sectoral coaxial ridged waveguides are shown. The formulas obtained in the section allow to compute cutoff wave numbers and electric and magnetic fields distributions of TE modes in the presence of the ridge either on the inner or the outer wall of the waveguide.

TM modes. The formulas obtained in the section allow to compute cutoff wave numbers and electric and magnetic fields distributions of TM modes in the presence of the ridge either on the inner or the outer wall of the waveguide.

Solutions convergence for cutoff wave numbers. The cutoff wave numbers convergence analysis depending on the amount of partial modes has been carried out. Residual errors plots for cutoff wave numbers computing of first four modes as dependences on the amount of partial modes are presented. It has been shown that it is enough to use 24 partial modes for the calculation of sectoral coaxial ridged waveguides cutoff wave numbers for both configurations by transverse field-matching technique with residual error less than 0.1%.

Conclusions. General conclusions of the paper are given.

***Keywords**: electrodynamics boundary problem, sectoral coaxial ridged waveguide, transverse field-matching technique, TE modes, TM modes, solutions convergence, residual error.*